

# Uncorrected Proof

## Control of failure of lap shear epoxy adhesive joint through CNTs

Anurag Mishra<sup>1\*</sup>, Akhilesh Singh<sup>1</sup>, Deep Narayan Maurya<sup>2</sup>, B.S Yadav<sup>3</sup>, Abhishek Singh<sup>4</sup>,  
Ashutosh Singh<sup>1</sup>,

1. Department of Chemistry, K. S. Saket P.G. College Ayodhya, India, 224123
2. Department of Chemistry, D.N. College Meerut, India, 250002
3. Department of Physics, D.N. College Meerut, India, 250002
4. Department of Chemistry, Up Autonomous College, Varanasi, India, 221002

\*Corresponding author: (anuragm878@gmail.com)

### Abstract:

In this research investigation, we explore the attributes of lap shear connections, employing epoxy adhesive and a carbon nanotube-epoxy nanocomposite on a mild steel substrate. We offer an intricate portrayal of a variety of factors, encompassing the surface characteristics of mild steel, the width of the adhesive bonding layer (thickness), the affinity in term of wettability between epoxy resin as adhesive and mild steel substrate surface, and the impact of carbon nanotube (CNT) incorporation within the epoxy resin. These variables collectively exert a significant influence on sustainability of lap shear joints under stress. Our empirical findings underscore a noteworthy enhancement in the lap shear joint's strength, attributed to the even dispersion of CNTs within the polymer matrix, with consequent modifications in the surface of substrate. Furthermore, these alterations induce a shift in the failure mode exhibited by lap shear connections. Remarkably, the introduction of 0.5 weight percent of CNTs into the epoxy adhesive emerges as the most substantial contributor to the augmentation in lap shear strength

**Keywords:** CNTs, Mild Steel, Epoxy, Adhesive, Lap shear joints.

### Introduction:

Epoxy constitutes a two-component system resulting from a cross-linking reaction, commonly known as curing, between epoxide groups in one component and nucleophile groups in the second component. The presence of this cross-linking network transforms epoxy into a

thermosetting polymer with commendable mechanical and thermal properties. Nonetheless, this cross-linking imparts a brittle nature to epoxy, which limits its applicability.

Depending on the degree of cross-linking, epoxy can exhibit a wide range of properties, including respectable tensile performance, minimal shrinkage during curing, strong chemical resistance, high anti-corrosion properties, environmental resilience, dimensional stability, and excellent adhesion [1–7]. Epoxy finds extensive use as an adhesive in the automobile and aircraft industries, as an electrical insulating material in the electric and electronics sectors, as a coating material, and in composite materials [1-7]. Epoxy-based adhesive offers numerous advantages in comparison of other adhesive like even stress distribution, the ability to bond different material surfaces, effective sealing, and relatively low weight compared to mechanical fastenings [8]. However, the brittle nature of epoxy limits its application, particularly in metal adhesive joints, due to lower resistance to crack propagation [9–11].

To boost the performance of epoxy, it has become common practice to incorporate various nano-fillers, resulting in epoxy nanocomposites with promising potential for bonding diverse components. These nanocomposites demonstrate improvements in key properties like increased modulus, thermal stability, toughness, and strength [12–15]. Carbon nanotubes (CNTs), among the favored nano-fillers for epoxy, are notable for their ability to improve physical, mechanical, electrical, anti-corrosion, and adhesive [16–24]. However, the literature on the impact of CNTs on epoxy-based joints remains somewhat limited. The effectiveness of a nano fillers reinforced adhesive depends on various factors, including the even dispersion of nano fillers, adherent material thickness, substrate surface topography, adhesive bond line thickness, and the adhesive's ability to wet the substrate.

Historically, diverse methods such as in-situ polymerization, extrusion, ball milling, melt milling, electrospinning, surface modification of fillers, and ultrasonic mixing have been employed to achieve a uniform and agglomerate-free dispersion of nano fillers. This uniform dispersion significantly enhances the nanocomposite's performance [25–33].

Furthermore, mechanical polishing and chemical reaction on metallic substrate have been applied to improve the wettability and joint strength between the adhesive and the metallic substrate [34–37]. An appropriate surface roughness on the substrate contributes positively to adhesive performance by providing a larger surface area for mechanical interlocking between the adhesive and substrate [38]. Mechanical treatments serve a dual purpose, eliminating surface contaminants such as greases, dust, oils and oxides layers while simultaneously imparting surface roughness, leading to increased bond strength. The temperature and duration of reaction that generates cross linking network (epoxy curing of epoxy) also significantly affect the performance of joint[37, 38]. In the realm of adhesives, the width of the adhesive layer between substrate, (also called bond line thickness), emerges as a critical factor influencing joint strength, primarily due to the relatively brittle nature of neat epoxy.

However, the relationship between strength of join and thickness of joint remains a subject of ongoing investigation. In contrast to classical analyses, experimental observations suggest that joint performance may not necessarily improve with an increase in bond line thickness [39, 40]. Consequently, there is a pressing need for a more comprehensive understanding of how the wettability of epoxy and CNT-epoxy nanocomposites on the substrate, bond line thickness (width of joint), and different substrate surface morphologies collectively influence joint strength.

## **2. Experimental:**

### **2.1 Materials:**

Lap joints were constructed using mild steel strips, which are commercially available with a thickness of 2.2 mm. Two types of adhesives were employed in the fabrication process: neat epoxy and a CNT-epoxy nanocomposite. The CNTs utilized in this research are multi-walled carbon nanotubes (MWCNTs) (Diameter -38 nm), as illustrated in Figure 1. These MWCNTs were synthesized through the chemical vapor deposition method. Additionally, the adhesive consisted of resin and an aliphatic hardener obtained from Huntsman Company, serving as the base material for the adhesive.

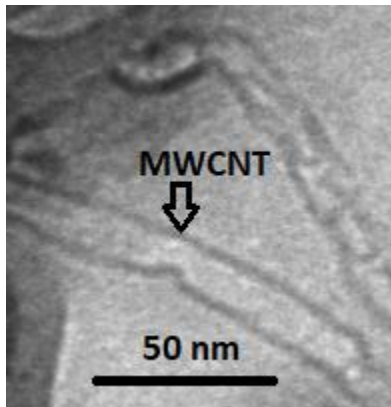


Figure1. TEM image of MWCNT

## 2.2 Preparation of mechanically and chemically treated surfaces of mild steel substrate:

Surface modification of the substrate involved both mechanical polishing and chemical procedures to ensure proper preparation:

**Mechanical Treatment:** To prepare the faying surface, a mechanical process was employed, involving the use of 220-grade emery paper for polishing [41]. This procedure was carried out to remove any contaminants such as metal oxides, dirt, and grease.

**Chemical Treatment:** A chemical treatment procedure adhering to the ASTM D2651 standard was followed. In this process, a strip of substrate was immersed for 3 minutes in a solution (10 wt.%  $\text{H}_2\text{SO}_4$  and 10 wt.% oxalic acid in water). Subsequently, the steel strip underwent a rinsing step with deionized (DI)  $\text{H}_2\text{O}$  for 4 minutes. To maintain surface pH at 7 (Neutralization) the, a solution containing NaOH (2 wt.%) was utilized. Following this, the surface was thoroughly rinsed with tap  $\text{H}_2\text{O}$  and then dried at a temperature of  $65^\circ\text{C}$ .

**Characterization of Treated Surfaces:** The prepared surfaces of the substrate, which underwent both mechanical and chemical treatments, were examined using a Field Emission Scanning Electron Microscope (FESEM) operating at an accelerated voltage of 15 kV. Additionally, to assess the substrate surface roughness, a Mitutoyo SJ 400 profilometer was employed.

## 2.3 Preparation of different adhesives namely neat epoxy and CNT-epoxy nanocomposite:

**Neat epoxy:** Initially, an amine-based hardener was introduced into the resin (10 wt.%). The two components were meticulously mixed using a glass rod, and subsequent vacuum degassing was

performed to eliminate any trapped air. The resulting adhesive, composed of neat epoxy, was then utilized to fabricate adhesive joints for mild steel, as depicted in Figure 2.

### **CNT-epoxy nanocomposite:**

To formulate the CNT-epoxy nanocomposite adhesive, the following procedure was meticulously followed:

Initially, CNTs (0.5 wt.%) were mixed into the resin. To reduce the mixture's viscosity, 15 wt.% of acetone was introduced, and thorough mixing of the two components was achieved using a glass rod. Ultrasonic waves were then employed, generated by a Vibracell ultrasonic processor, for a duration of 60 minutes at 70% amplitude, utilizing a pulse cycle (10 seconds on and 10 seconds off) to ensure the dispersion of CNTs, as illustrated in Figure 2. Following the ultrasonic treatment, the mixture was maintained at 50°C to facilitate the vaporization of acetone.

Subsequently, the hardener (10 wt.%) was evenly blended into the mixture, followed by and vacuum degassing to eliminate any trapped air. The resulting CNT-epoxy nanocomposite adhesive was then employed in the creation of adhesive joints.

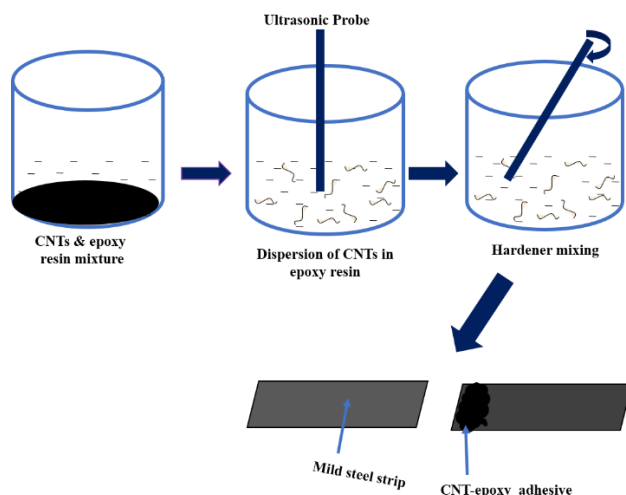


Figure 2. An outlined diagram depicting the process employed in the preparation of CNT-epoxy nanocomposite adhesive.

### **2.4 Fabrication of Joints:**

Lap shear joints were meticulously fabricated on mild steel substrates utilizing two distinct types of adhesives: neat epoxy adhesive and CNT-epoxy nanocomposite adhesive (shortly called CNT-epoxy Adhesive), adhering to the procedural guidelines outlined in the ASTM D1002 standard.

The adhesives were evenly spread across both surfaces of the mild steel substrate to ensure complete coverage and optimal adhesion. These prepared surfaces were then joined together following the configuration illustrated in Figure 3. Throughout the assembly of adhesive joints, varying rolling loads (3 N, 6 N, 9 N, and 12 N) were applied (1.5 mm/min) to achieve different bond line thicknesses (width of joint).

Subsequent to the assembly, the joints were placed within an oven set at 70°C for a curing duration of 10 hours. After curing, any excess adhesive protruding beyond the joints was meticulously removed to prevent compromising the integrity of the joints. The width of joints was subsequently recorded utilizing an optical microscope.

To assess the performance of the joints under tensile stress, single lap shear testing was conducted employing a Hounsfield H25K-S machine (Cross-head speed of 0.5 mm/min). The specimens of joints were securely held in position using alignment tabs, as depicted in Figure 3. The lap shear strength ( $\sigma_s$ ) of the adhesive joints, employing different adhesive types, was determined using the formula  $\sigma_s = (N/X) \times Y$ , (N - failure load in Newtons, X- bond line thickness in millimeters, and Y - length of joint in millimeters). The results reported here are the averages obtained from a minimum of four measurements, and a stress-strain plot was recorded until the adhesive joint reached the point of fracture.

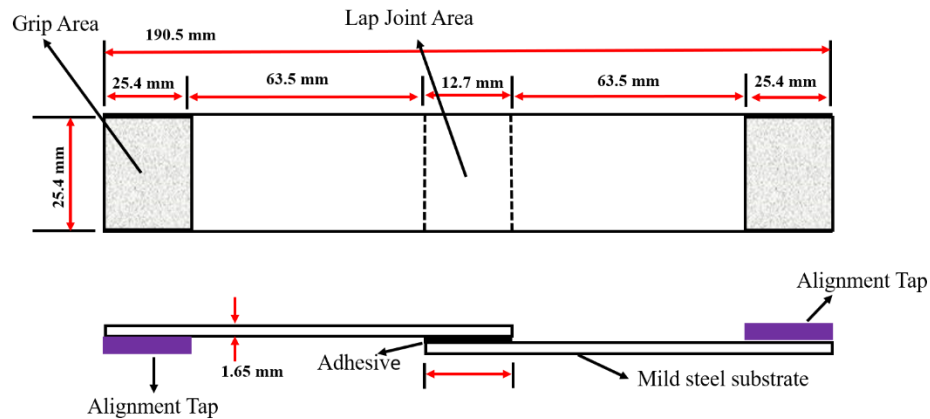


Figure3.Dimensions of a single lap adhesive joint.

### 3. Results and discussion:

#### 3.1 Mechanical and chemical treated surfaces:

Figure 4 displays FESEM images of the mild steel substrate, providing a comparison between surfaces prepared through mechanical polishing and chemical treatment at both low and high magnifications. In Figure 4(a), we can observe the effects of mechanical polishing, which results

in parallel scratches with hills and valleys structure on substrate's surface. Conversely, Figure 4(b) demonstrates the impact of chemical treatment applied on substrate after mechanically polishing, which introducing porosity through a chemical reaction within the areas corresponding to the hills and valleys.

The chemical reaction responsible for etching the mild steel substrate involves acidic action. This reaction causes positively charged Fe ions to be released into the aqueous solution from metallic Iron, leading to the creation of surface roughness in the form of porosity. This transformation is clearly evident in Figure 4(b). The roughness measurements for both type surfaces were determined to be  $R_a = 0.3 \text{ mm}$  and  $R_z = 2.5 \text{ mm}$ , respectively. These measurements align with the observations derived from the FESEM images presented in Figure 4.

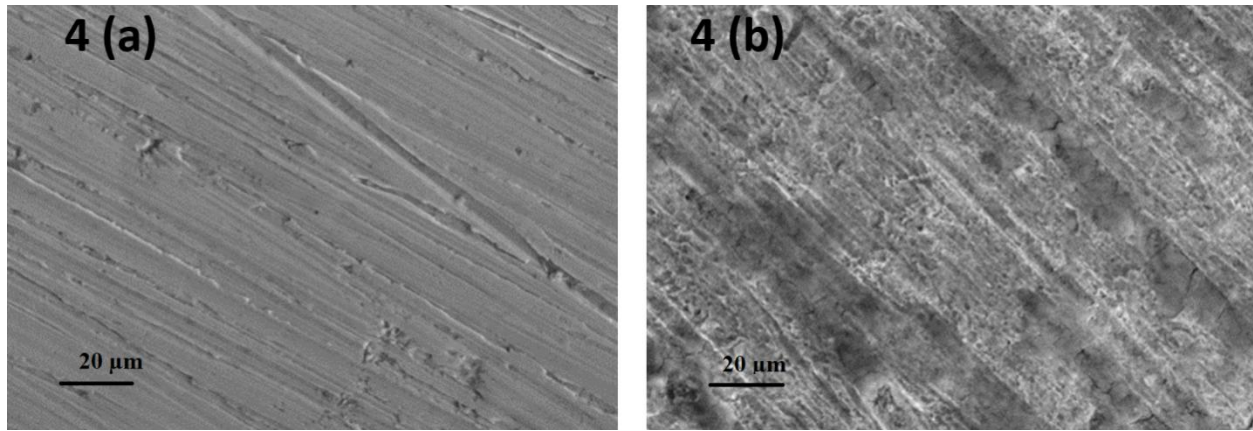


Figure 4. FESEM images 4(a)mechanically and4(b) chemically treatedmild steel substrates.

### 3.2 Wettability:

The wettability of an adhesive on a substrate (Mild Steel) is a crucial factor that significantly influences the performance of a lap shear joints. In our investigation, we explored the wettability of epoxy-based adhesive towards various surfaces, including mechanically polished surface with neat epoxy, chemically modified surface with neat epoxy, and chemically modified surface with CNT-epoxy adhesive (0.5 wt.%).

To assess the wettability of these adhesives, we measured the contact angle. As depicted in Figure 5, the contact angles ( $\theta$ ) for different adhesives on these distinct surfaces were as follows: mechanically polished surface exhibited a contact angle of  $65^\circ$  with neat epoxy, while chemically modified surface had a lower contact angle of  $58^\circ$  with neat epoxy. This indicates that chemical reaction of iron with acidic solution enhances the wettability of neat epoxy on

substrate in comparison to mechanically polishing alone. However, the chemically modified surface with CNT-epoxy adhesive (0.5 wt.%) exhibited an even lower contact angle of  $52^\circ$ , which further affirms the enhancement in epoxy wettability attributed to the presence of CNTs.

The chemical reaction of iron with acidic solution creates a porous structure on the surface, facilitating mechanical interlocking and offering a larger adhesive area with improved surface wettability. These observations suggest that the performance of adhesive joints may be influenced by surface structure, available adhesive area, and wettability. Additionally, the presence of chemical forces between the substrate surface and the epoxy can also play an important role in deciding the performance of joints. Therefore, it is essential to investigate the lap shear strength as a function of bond line thickness (width of joint). It is noteworthy that the viscosity of epoxy-based adhesive can affect its flow properties, but in our study, we observed no significant alteration in viscosity, especially with the very low loading of CNTs (0.5 wt.%) in the epoxy-based adhesive.

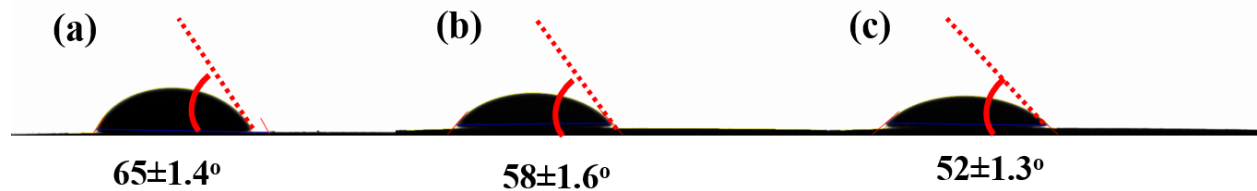


Figure 5. Depicts photographs illustrating the contact angles of different adhesive scenarios: (a) Contact angle for neat epoxy/mechanically polished surface. (b) Contact angle for neat epoxy/chemically modified surface. (c) Contact angle for 0.5 wt.% CNT-epoxy/chemically modified surface

**3.3 Effect of width of joint on lap shear strength for neat epoxy/mechanically polished surface:** Table 1 provides valuable insights into the influence of applied rolling load during joint fabrication on the width of joints for neat epoxy applied to mechanically polished substrates (Mild steel), along with the corresponding lap shear strength. This table underscores the significant impact of the magnitude of rolling load on width of joints.

The table demonstrates that as the applied weight increases, reaching up to 9 Newtons (N), the width of joints experiences a noticeable decrease, followed by a more gradual reduction as the load continues to increase. This phenomenon suggests that at thickness (width) levels below 90



$\mu\text{m}$ , the interfacial drag force exerted by the substrate surface becomes increasingly effective in securing the epoxy-based adhesive in place, thereby limiting its flow under the applied rolling load.

Table 1 also provides insight into how the width of neat epoxy adhesive between the substrates influences the strength of joints on mechanically polished substrates. An interesting trend is evident: as the width decreases, up to  $90\ \mu\text{m}$ , the laps shear strength increases. However, with a further decrease in width of joints, the strength experiences a significant decline. This reduction in lap shear strength at lower adhesive width can be attributed to the relatively higher brittleness of neat epoxy, making it susceptible to tearing due to surface tension, which can disrupt its continuity within the adhesive joint. On the other hand, higher width of joints increases the likelihood of joint fracture by altering the triaxial stress distribution and potentially creating micro defects, such as air entrapment, within the adhesive joint.

These observations underscore the intricate relationship between adhesive width between the substrate (thickness), substrate treatment, and lap shear strength, offering insights into the optimal conditions for achieving robust adhesive joints.

Table 1. Width of joints and Lap shear strength of neat epoxy adhesive for mechanically polished substrate

Rolling load (N)	Adhesive/surface	Width of Joints ( $\mu\text{m}$ )	Lap shear Strength (MPa)
3	Neat Epoxy/mechanically polished	152	3.1 ( $\pm 0.720$ )
6	Neat Epoxy/mechanically polished	125	4.2 ( $\pm 0.837$ )
9	Neat Epoxy/mechanically polished	90	5.9 ( $\pm 0.989$ )
12	Neat Epoxy/mechanically polished	77	3.4 ( $\pm 2.126$ )

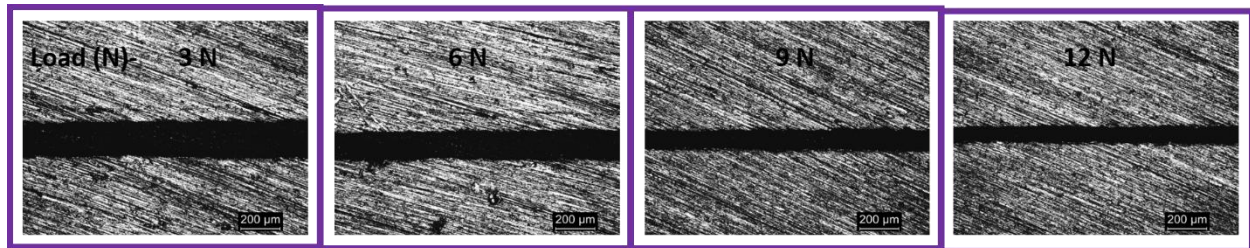


Figure 6. Optical micrographs depicting the width of neat epoxy adhesive joints on mechanically polished substrate for various load.

### 3.3 Determining shear failure modes in epoxy-based adhesive:

In polymer adhesive joints, there are typically two primary modes of failure:

1. Cohesive Failure: In this mode, crack propagation occurs within the polymer-based adhesive itself. Cohesive failure is characterized by the presence of polymeric material on both faying surfaces of the substrate after the joint has failed.
2. Adhesive Failure: In this mode, crack propagation takes place along the interface between the polymer-based adhesive and substrate. Adhesive failure is characterized by one faying surface of the substrate being entirely covered by polymer, while the other faying surface lacks polymer coverage.

It's important to note that adhesive failure is typically observed in joints where neat epoxy is used with mechanically polished substrates. In such cases, only one of the faying surfaces is completely covered with neat epoxy, while the other faying surface primarily exposes the substrate surface, as confirmed in Figure 9.

In contrast, for joints involving chemically modified substrates, cohesive failure is observed, as also confirmed in Figure 9. Therefore, it becomes evident from figure 9 results that acidic action on polished substrates swings the failure mode towards cohesive failure from adhesive failure, leading to an improvement in the strength (Table 2). This shift can be primarily attributed to the higher wettability of neat epoxy on chemically modified substrates (Figure 5) and the introduction of porosity on the surface (as shown in Figures 4(b)), which facilitates mechanical interlocking and ultimately improves the lap shear strength of joints. The location of shear failure in joints is determined by the weaker of the two components: the adhesive itself and the interfacial bond between substrate and adhesive. Notably, the interfacial strength experiences significant improvement through chemical reaction applied to the metal substrate, as evident in Figure 9.

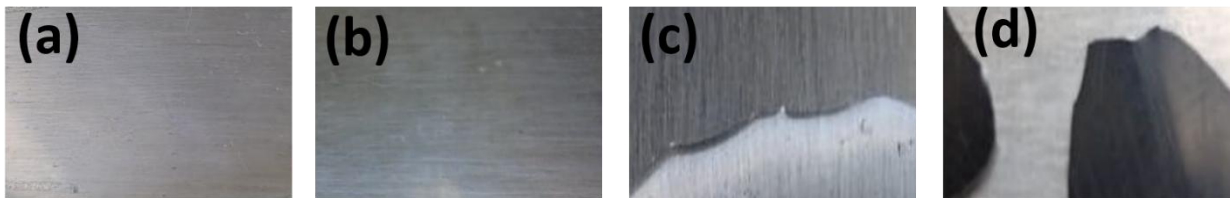


Figure 9. Typical fracture surfaces of (a) Mechanically polished substrate without epoxy (b) Mechanically polished substrate with epoxy (c) Chemically modified substrate with epoxy (d) Chemically modified substrate with CNT-epoxy.

### **3.4 Lap shear strength of neat epoxy and CNT-epoxy adhesives on chemically modified surface:**

Our current research focus revolves around enhancing the strength of epoxy-based adhesives. To accomplish this goal, we reinforced 0.5 weight percentages of carbon nanotubes into the epoxy adhesive. This nanocomposite was formed by uniformly dispersing CNTs within the cross-linking network of epoxy using ultrasonic waves, as illustrated in Figure 2. Subsequently, we evaluated the strength of the resulting CNT-epoxy nanocomposites as adhesive when used on chemically modified substrates.

Throughout our study, we maintained a consistent bond line thickness (width of joint) of approximately 90  $\mu\text{m}$ . This specific width of joint was determined to yield the maximum strength for joints when employing neat epoxy as adhesive on mechanically polished substrates. The impact of varying CNT loading in the epoxy adhesive is visualized in Figure 10 and summarized in Table 2 for chemically modified substrates. This investigation seeks to provide insights into the influence of CNT loading on the adhesive's performance under these specific conditions.

The data from Figure 10 and Table 2 reveals a clear trend: as 0.50 wt.% of CNTs loaded in the epoxy adhesive, the strength of joints on chemically modified substrates experiences a noticeable improvement. The fracture behavior of CNT-epoxy adhesive joints is characterized by a mixed mode of failure, predominantly involving cohesive failure within the CNT-epoxy nanocomposite. In this mode, cracks propagate through the CNT-epoxy material, followed by interfacial fracture, as indicated by Figure 9.

By examining the cohesive failure zone of neat epoxy on chemically modified substrates through FESEM images (Figure 11(a)), we observe that cracks propagate smoothly and freely, creating river-like structure. This signifies the inherent brittleness of the epoxy, which cannot effectively resist crack propagation, resulting in typical brittle fracture.

The rise in strength with 0.50 wt.% CNT loading in epoxy can be attributed to the homogeneous and cluster-free dispersion of CNTs, as observed in Figure 11(b). This dispersion results in a rougher fracture surface, as evident from Figure 11(b), with numerous circuitous pathways. A rougher surface dissipates more energy during fracture, leading to increased strength. In this case, CNTs resist cohesive fracture by deflecting crack growth through crack blunting mechanisms within the matrix. Additionally, the slightly improved wettability of CNT-epoxy on chemically modified surfaces also contributes positively to the strength enhancement of joints.

Table 2 Summarizes the strength of adhesives.

Rolling load (N)	Adhesive/surface	Width of joints ( $\mu\text{m}$ )	Lap shear Strength (MPa)
9	Neat Epoxy/mechanically polished	90	5.9 ( $\pm 0.989$ )
9	Neat Epoxy/chemically modified	88	7.5 ( $\pm 0.798$ )
9	CNT-Epoxy/chemically modified	88	10.2 ( $\pm 1.112$ )

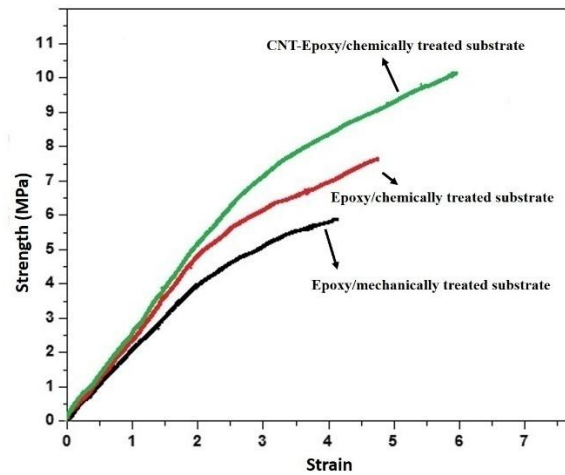


Figure 10. Lap Shear Strength vs strain curves for various combination of adhesive with substrate.

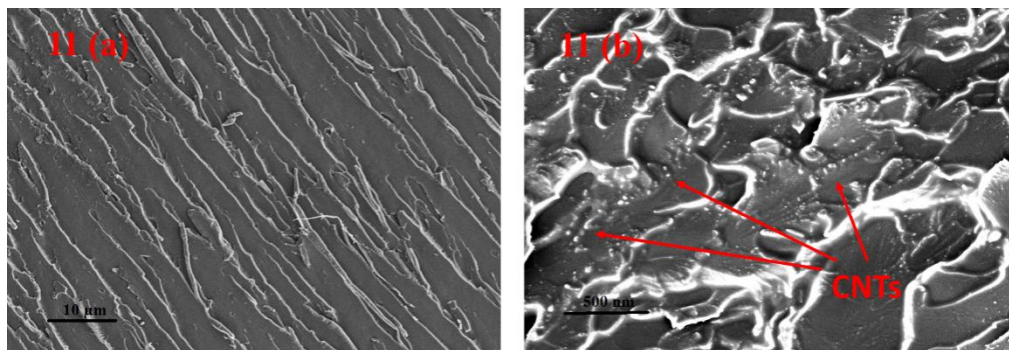


Figure 11. Cohesive failure zone (a) Neat Epoxy (b) CNT-epoxy on chemically modified substrate (FESEM)

**Conclusion** The strength of an adhesive is intricately tied to two critical factors: the surface characteristics of substrates and the width of joints. The application of acid treatments to metal

substrate has the capacity to transform the failure mode from adhesive to cohesive failure, resulting in higher strength of joints.

When CNTs are dispersed uniformly and without clustering within the polymer-based adhesive, they significantly enhance strength. This enhancement is accompanied by a mixed mode of failure observed during testing.

## References:

- [1] A.K. Hamzat, A.Y. Adesina, T. Rasheed & M. A. Samad., Assessing the Tribological Behavior of Nanoclay-Reinforced Epoxy Coatings Under Dry Sliding and Seawater Lubricated Conditions. *J. of Materi Eng and Perform.*, 2023, **32**, p 6905–6914. <https://doi.org/10.1007/s11665-022-07605-7>
- [2] M. M. Liu, H. X. Hu, Z. B. Wang & Y. G. Jheng., Effect of Epoxy Sealant Loaded with Modified Montmorillonite on the Corrosion Resistance of Fe-Based Amorphous Metallic Coating. *J. of Materi Eng and Perform.*, 2023, **32**, p 7593–7610. <https://doi.org/10.1007/s11665-022-07669-5>
- [3] Z. B. Wang, Z. Y. Wang, H. X. Hu, C. B. Liu & Y. G. Zheng., Corrosion Protection Performance of Nano-SiO<sub>2</sub>/Epoxy Composite Coatings in Acidic Desulfurized Flue Gas Condensates. *J. of Materi Eng and Perform.*, 2016, **25**, 3880–3889. <https://doi.org/10.1007/s11665-016-2212-3>
- [4] R. Vasireddi & D. R. Mahapatra., Micro-crack Pinning and Interfacial Fracture in Mixed Metal Oxide Reinforced Epoxy Nanocomposite. *J. of Materi Eng and Perform.*, 2018, **27**, 5938–5946. <https://doi.org/10.1007/s11665-018-3698-7>
- [5] R. C. L. Tai & Z. Szklarska-Smialowska., Effect of fillers on the degradation of automotive epoxy adhesives in aqueous solutions - Part II The microhardness change and delamination of automotive epoxy adhesives in distilled water and NaCl solutions. *J. of Mater Sci.*, 1993, **28**, p 6205–10. doi:10.1007/BF00365045.
- [6] R. Kahraman & M. Al-Harthi., Moisture diffusion into aluminum powder-filled epoxy adhesive in sodium chloride solutions. *Int. J. of Adhes Adhes.*, 2005, **25**, p 337–41. doi:10.1016/j.ijadhadh.2004.10.003.
- [7] S. A. Kumar, M. Alagar & V. Mohan., Studies on corrosion-resistant behavior of siliconized epoxy interpenetrating coatings over mild steel surface by electrochemical methods. *J. of Materi Eng and Perform.*, 2002, **11**, 123–129. <https://doi.org/10.1361/105994902770344178>.
- [8] S. D. Thoppul, J. Finegan & R. F. Gibson., Mechanics of mechanically fastened joints in polymer-matrix composite structures - A review. *Compos Sci Technol*, 2009, **69**, p 301–29. doi:10.1016/j.compscitech.2008.09.037.
- [9] R. J. Moulds & T. R. Baldwin., Toughened adhesives for structural applications. *Int. J. of Adhes Adhes.*, 1983, **3**, p 203–7. doi:10.1016/0143-7496(83)90095-7.
- [10] K. Kumar, P. K. Ghosh, A. Kumar & O. Singh., Enhanced Thermomechanical Properties of ZrO<sub>2</sub> Particle Reinforced Epoxy Nanocomposite. *J. of Materi Eng and Perform.*, 2021, **30**, p 145–153. <https://doi.org/10.1007/s11665-020-05350-3>
- [11] A. Ozel, B. Yazici, S. Akpinar, M. D. Aydin & Ş. A. Temiz., study on the strength of adhesively bonded joints with different adherends. *Compos Part B Eng.*, 2014, **62**, p 167–74. doi:10.1016/j.compositesb.2014.03.001.
- [12] N. C. Adak, S. Chhetri, N. H. Kim, N. C. Murmu, P. Samanta & T. Kuila., Static and

Dynamic Mechanical Properties of Graphene Oxide-Incorporated Woven Carbon Fiber/Epoxy Composite. *J. of Materi Eng and Perform.*, 2018, **27**, p 1138–1147. <https://doi.org/10.1007/s11665-018-3201-5>

- [13] S. Kirtania & D. Chakraborty., Determination of Thermoelastic Properties of Carbon Nanotube/Epoxy Composites Using Finite Element Method. *J. of Materi Eng and Perform.*, 2018, **27**, p 3783–3788. <https://doi.org/10.1007/s11665-017-2981-3>
- [14] R. Mactabi, I. D. Rosca & S. V. Hoa., Monitoring the integrity of adhesive joints during fatigue loading using carbon nanotubes. *Compos Sci Technol*, 2013, **78**, p 1–9. doi:10.1016/j.compscitech.2013.01.020.
- [15] J. H. Tang, I. Sridhar & N. Srikanth., Static and fatigue failure analysis of adhesively bonded thick composite single lap joints. *Compos Sci Technol.*, 2013, **86**, p 18–25. doi:10.1016/j.compscitech.2013.06.018.
- [16] J. J. Karippal, H. N. Narasimha Murthy, K. S. Rai, M. Krishna & M. Sreejith., Electrical and Thermal Properties of Twin-Screw Extruded Multiwalled Carbon Nanotube/Epoxy Composites. *J. of Materi Eng and Perform.*, 2010, **19**, p 1143–1149. <https://doi.org/10.1007/s11665-010-9604-6>
- [17] J. Shen, W. Huang, L.Wu, Y. Hu & M. Ye., The reinforcement role of different amino-functionalized multi-walled carbon nanotubes in epoxy nanocomposites. *Compos Sci Technol.*, 2007, **67**, p 3041–50. doi:10.1016/j.compscitech.2007.04.025.
- [18] A. Montazeri A & M. Chitsazadeh., Effect of sonication parameters on the mechanical properties of multi-walled carbon nanotube/epoxy composites. *Mater Des.*, 2014, **56**, p 500–8. doi:10.1016/j.matdes.2013.11.013.
- [19] V. Jain, A. Bisht, S. Jaiswal, K. Dasgupta & D. Lahiri., Assessment of Interfacial Interaction in Graphene Nanoplatelets and Carbon Fiber-Reinforced Epoxy Matrix Multiscale Composites and Its Effect on Mechanical Behavior. *J. of Materi Eng and Perform.*, 2021, **30**, p 8913–8925. <https://doi.org/10.1007/s11665-021-06115-2>
- [20] F. Gardea & D. C. Lagoudas., Characterization of electrical and thermal properties of carbon nanotube/epoxy composites. *Compos Part B Eng.*, 2014, **56**, p 611–20. doi:10.1016/j.compositesb.2013.08.032.
- [21] D. Zeng, Z. Liu, Z., S. Bai, J. Zhao & J. Wang., Corrosion Resistance of Bis-Silane-Modified Epoxy Coatings on an Al-Zn-Mg-Cu Alloy. *J. of Materi Eng and Perform.*, 2020, **29**, p 5282–5290. <https://doi.org/10.1007/s11665-020-05049-5>
- [22] W. Shen, L. Feng, X. Liu, H. Luo, Z. Liu, P. Tong & W. Zhang., Multiwall carbon nanotubes-reinforced epoxy hybrid coatings with high electrical conductivity and corrosion resistance prepared via electrostatic spraying. *Prog Org Coatings.*, 2016, **90**, p 139–46. doi:10.1016/j.porgcoat.2015.10.006.
- [23] N. W. Khun, B. C. R. Troconis & G. S. Frankel., Effects of carbon nanotube content on adhesion strength and wear and corrosion resistance of epoxy composite coatings on AA2024-T3. *Prog Org Coatings.*, 2014, **77**, p 72–80. doi:10.1016/j.porgcoat.2013.08.003.
- [24] S. Yu, M. N. Tong & G. Critchlow., Use of carbon nanotubes reinforced epoxy as adhesives to join aluminum plates. *Mater Des.*, 2010, **31**, p S126–9. doi:10.1016/j.matdes.2009.11.045.
- [25] N. G. Sahoo, S. Rana, J. W. Cho, L. Li & S. H. Chan., Polymer nanocomposites based on functionalized carbon nanotubes. *Prog Polym Sci.*, 2010, **35**, p 837–67. doi:DOI 10.1016/j.progpolymsci.2010.03.002.

- [26] J. Zhang, S. Ju, D. Jiang & H. X. Peng., Reducing dispersity of mechanical properties of carbon fiber/epoxy composites by introducing multi-walled carbon nanotubes. *Compos Part B Eng.*, 2013, 54, p 371–6. doi:10.1016/j.compositesb.2013.05.046.
- [27] J. B. Bai & A. Allaoui., Effect of the length and the aggregate size of MWNTs on the improvement efficiency of the mechanical and electrical properties of nanocomposites - Experimental investigation. *Compos Part A Appl Sci Manuf.*, 2003, 34, p 689–94. doi:10.1016/S1359-835X(03)00140-4.
- [28] L. S. Schadler, S. C. Giannaris & P. M. Ajayan., Load transfer in carbon nanotube epoxy composites. *Appl Phys Lett.*, 1998, 73, p 3842–4. doi:10.1063/1.122911.
- [29] S. Cui, R. Canet, A. Derre, M. Couzi & P. Delhaes., Characterization of multiwall carbon nanotubes and influence of surfactant in the nanocomposite processing. *Carbon N Y.*, 2003, 41, p 797–809. doi:10.1016/S0008-6223(02)00405-0.
- [30] L. Ci & J. Bai., The reinforcement role of carbon nanotubes in epoxy composites with different matrix stiffness. *Compos Sci Technol.*, 2006, 66, p 599–603. doi:10.1016/j.compscitech.2005.05.020.
- [31] P. Laborde-Lahoz, W. Maser, T. Martinez, A. Benito, T. Seeger, P. Cano, R. Guzman de Villoria & A. Miravete., Mechanical Characterization of Carbon Nanotube Composite Materials. *Mech Adv Mater Struct.*, 2005, 12, p 13–9. doi:10.1080/15376490590491792.
- [32] G. Gkikas, N. M. Barkoula & A. S. Paipetis., Effect of dispersion conditions on the thermo-mechanical and toughness properties of multi walled carbon nanotubes-reinforced epoxy. *Compos Part B Eng.*, 2012, 43, p 2697–705. doi:10.1016/j.compositesb.2012.01.070.
- [33] J-P Jeandrou, C. Peyrac, F. Lefebvre, J. Renard, V. Gantchenko, B. Patamaprohm & C. Guinault., Fatigue Behaviour of Adhesive Joints. *Procedia Eng.*, 2015, 133, p 508–17. doi:10.1016/j.proeng.2015.12.622.
- [34] P. K. Ghosh, K. Kumar & A. Kumar., Studies on Thermal and Mechanical Properties of Epoxy-Silicon Oxide Hybrid Materials. *J. of Materi Eng and Perform.*, 2015, 24, p 4440–4448. <https://doi.org/10.1007/s11665-015-1719-3>.
- [35] G. M. Wu, Y. T. Shyng, S. F. Kung & C. F. Wu., Oxygen plasma processing and improved interfacial adhesion in PBO fiber reinforced epoxy composites. *Vacuum.*, 2009, 83, p S271–4. doi:10.1016/j.vacuum.2009.01.080.
- [36] B. R. K. Blackman, A. J. Kinloch & J. F. Watts., The plasma treatment of thermoplastic fibre composites for adhesive bonding. *Composites.*, 1994, 25, p 332–41. doi:10.1016/S0010-4361(94)80003-0.
- [37] V. Cooper, A. Ivankovic, A. Karac, D. McAuliffe & N. Murphy., Effects of bond gap thickness on the fracture of nano-toughened epoxy adhesive joints. *Polym (United Kingdom).*, 2012, 53, p 5540–53. doi:10.1016/j.polymer.2012.09.049.
- [38] S. Azari, M. Papini & J. K. Spelt., Effect of adhesive thickness on fatigue and fracture of toughened epoxy joints - Part I: Experiments. *Eng Fract Mech.*, 2011, 78, p 153–62. doi:10.1016/j.engfracmech.2010.06.025.
- [39] D. M. Gleich, M. J. L. Van Tooren & A. Beukers., Analysis and evaluation of bondline thickness effects on failure load in adhesively bonded structures. *J Adhes Sci Technol.*, 2001, 15, p 1091–101. doi:10.1163/156856101317035503.
- [40] L. D. R. Grant, R. D. Adams & L. F. M. da Silva., Experimental and numerical analysis of single-lap joints for the automotive industry. *Int J Adhes Adhes.*, 2009, 29, p 405–13. doi:10.1016/j.ijadhadh.2008.09.001.

- [41] A. M. Pereira, P. N. B. Reis, J. A. M. Ferreira & F. V. Antunes., Effect of saline environment on mechanical properties of adhesive joints. *Int J Adhes Adhes.*, 2013, 47, p 99–104. doi:10.1016/j.ijadhadh.2013.08.002